Available online at www.sciencedirect.com
SCIENCE DIRECT
Biochimica et Biophysica Acta 1762 (2006) 304–311
BIOCHIMICA ET BIOPHYSICA ACTA
BBA
http://www.elsevier.com/locate/bba

A study of the nuclear trafficking of the splicing factor protein PRPF31 linked to autosomal dominant retinitis pigmentosa (ADRP)

Susan E. Wilkie [a], Keith J. Morris [a], Shomi S. Bhattacharya [a], Martin J. Warren [b], David M. Hunt [a,*]

[a] *Institute of Ophthalmology, University College London, 11-43 Bath Street, London EC1V 9EL, UK*
[b] *Department of Biosciences, University of Kent, Canterbury, Kent CT2 7NJ, UK*

Received 17 May 2005; received in revised form 6 December 2005; accepted 6 December 2005
Available online 4 January 2006

Abstract

In this study the mechanism of nuclear importation of the splicing factor PRPF31 is examined and the impact of two disease-linked mutations, A194E and A216P, assessed. Using pull-down assays with GST-tagged importin proteins, we demonstrate that His-tagged PRPF31 interacts with importin β1 for translocation to the nucleus, with no requirement for importin α1. The A194E and A216P mutations have no affect on this interaction. Fluorescence recovery after photobleaching (FRAP) was used to estimate the rate of movement of EGFP-tagged PRPF31 into the nuclei of live cells. The kinetics indicated a two-component recovery process; a fast component with $\tau \sim 6$ s and a slow component with $\tau \sim 80$ s. The mutations affected neither component. We conclude that the two mutations have no negative effect on interaction with the nuclear importation machinery. Reduced mutant protein solubility resulting in an insufficiency of splicing activity in cells with a very high metabolic demand remains the most likely explanation for the disease pathology in ADRP patients.

Keywords: PRPF31; Retinitis pigmentosa; Nuclear transport; FRAP

1. Introduction

Retinitis pigmentosa (RP) is a clinically and genetically heterogeneous group of generally progressive diseases of the retina. Initially, only the rod cells of the scotopic system are affected but subsequently both peripheral and central cones used in bright light vision may be affected, often leading to complete blindness. Clinical manifestations include pigment deposition in the retina and attenuation of retinal blood vessels, with later depigmentation or atrophy of the RPE. With an incidence of 1 in 3500 of the population, inheritance may be X-linked, autosomal dominant or autosomal recessive. Mutations within six genes (*RHO*, peripherin/*RDS*, *RP1*, *NRL*, *CRX* and *FSCN2*) encoding proteins uniquely expressed in photoreceptor cells have been reported to cause autosomal dominant (AD) forms of the disease. However, not all ADRP genes show a restricted pattern of expression and a number of ubiquitously expressed genes have been linked to the disease, including the mRNA splicing factor genes *PRPF31* [1], *PRPC8* [2] and *HPRP3* [3]. An intriguing aspect to the association of these latter genes with retinal disease is the fact that splicing occurs in every cell of the body and the genes thus have a general housekeeping function, yet the disease pathology is restricted to the rod photoreceptors of the retina.

The splicing of pre-mRNA in the nucleus is catalysed by a large ribonucleoprotein complex, the spliceosome, consisting of the pre-mRNA substrate and several small nuclear ribonucleoproteins (snRNPs) together with splicing factors not integrated into snRNPs. Splicing of the vast majority of introns involves five snRNPs, U1, U2, U4, U5 and U6. Spliceosome assembly involves firstly the binding of U1 and U2 to the pre-mRNA substrate with the formation of a pre-splicing complex (complex A), followed by binding of a trimer of U4/U5+U6 to form the spliceosome proper (complex B).

Abbreviations: PRPF31, pre-RNA splicing protein factor 31; ADRP, autosomal dominant retinitis pigmentosa; EGFP, enhanced green fluorescent protein; GST, glutathione sulphotransferase

* Corresponding author. Tel.: +44 207 608 6820; fax: +44 207 608 6863.
E-mail address: d.hunt@ucl.ac.uk (D.M. Hunt).

0925-4439/$ - see front matter © 2005 Elsevier B.V. All rights reserved.
doi:10.1016/j.bbadis.2005.12.004

The *PRPF31* gene on chromosome 19q13.4 (RP11) encodes a 61-kDa protein (PRPF31, also known as splicing factor 61K [4]), which is an integral component of the U4/U6+U5 tri-snRNP. Interestingly the other two splicing factor proteins linked to ADRP (HPRP3 and PRPC8) are also components of the same tri-snRNP [5–7].

Our previous work has focused on the functional consequences of the two missense disease-causing mutations in PRPF31, A194E and A216P, originally reported by Vithana et al. [8]. Using a yeast complementation assay, we showed that the introduction of the human A216P mutation into the yeast orthologue PRP31p effects only a partial rescue, although the mutant protein appears to be non-toxic in yeast even when highly expressed. We also found no evidence for any dominant negative effect in terms of splicing efficiency or accuracy attributable to either mutation, although a recent study using rod opsin mini-genes [9] indicates that there may be a direct effect of mutant splicing factor on the efficiency of splicing for some introns but not for others. Nevertheless, protein localisation studies in mammalian cells transfected with His-tagged PRPF31 constructs show mislocation of the mutant proteins, with a substantial proportion in the cytoplasm rather than the nucleus [8]. Western analysis also demonstrated that less soluble PRPF31 protein was present in the nucleus. We therefore postulated that this could be due to a defect in the trafficking of the mutant proteins to the nucleus. Furthermore, we suggested that insufficiency of splicing function may be the origin of the pathology. To explain the limitation of pathology to the retina, we proposed that the functional insufficiency arising from mutations in PRPF31 is only revealed under conditions of elevated splicing demand. With the need to replenish disc proteins on a daily basis, such conditions will exist in rod photoreceptors and this may underlie the pathology.

In this study, we have examined the process whereby PRPF31 is trafficked within the cell and the effects of the two disease causing mutations A194E and A216P on this process. PRPF31 contains a classical nuclear localisation sequence (NLS) between residues 351 and 364 (^{351}RKKRGGRRYRKMKE^{364}), as first identified from computer prediction software [1] and subsequently confirmed by generation of a deletion mutant (ΔNLS) in which this 14-residue sequence was deleted [8]. Targeting to the nucleus involves interaction of this NLS with one of a family of importin proteins, which carries the protein to the nuclear envelope where interaction with Ran.GTP mediates transport through the pore into the nucleus (reviewed in [10]). Here, we show that purified PRPF31 interacts with importin β1, but that this interaction does not appear to be affected by the two mutations A194E or A216P. Moreover, the mutations do not appear to affect the rate of nuclear importation of PRPF31 in live cells. Thus, the protein mislocation reported earlier [8] is not due to a failure of the mutant proteins to interact with the nuclear importation machinery, but instead arises from reduced protein solubility.

2. Materials and methods

2.1. Reagents

Oligonucleotides used as PCR primers were purchased from Sigma-Genosys, Cambridge, UK. The nucleotide sequences of all primers used in this study may be obtained by application to the authors. Restriction enzymes were supplied by Promega, Southampton, UK. Except where otherwise stated, all other chemicals and reagents were purchased from Sigma-Aldrich, Poole, UK.

2.2. Plasmid construction

Full-length importin α cDNA was amplified from pRSET-hSRP1α [11] using primer pair 5′Impα/3′Impα, inserted into the TA cloning vector pGEM.Teasy (Promega, Southampton, UK) and then transferred as a *Bam*HI–*Eco*RI digest fragment into the expression vector pGEX6P-1 (Amersham Biosciences, Little Chalfont, UK) to generate the construct pGEX-Impα. Full-length importin β cDNA was amplified similarly from the plasmid pET30.Impβ [12] using primers 5′Impβ/3′Impβ and then inserted as a *Bam*HI–*Xho*I digest fragment into pGEX6P-1 to yield the construct pGEX-Impβ.

The full-length wild type PRPF31 coding sequence was amplified from pTriEx.PRPF31.His using primers EGFPN1F (*Bgl*II-tagged) and EGFPN1R (*Xho*I/*Eco*RI-tagged) and inserted into pEGFP-N1 (Clontech, Basingstoke, UK) via the *Bgl*II and *Eco*RI sites to yield the construct pPRPF31-EGFP. Mutant versions of this construct containing the substitutions A194E and A216P were generated by removing the *Hin*dIII–*Xho*I digest fragment from pPRPF31-EGFP and replacing it with corresponding fragments from mutant versions of pTriEx.PRPF31.His.

2.3. Purification of wild type His-tagged PRPF31 expressed in HEK 293T cells

HEK 293T cells (ECACC) were transiently transfected with pTriEx.PRPF31.His in 135 mm diameter tissue culture dishes using the GeneJuice transfection reagent (Merck Biosciences Ltd., Nottingham, UK). Cells were harvested 48 h later, washed 3× with phosphate buffered saline (PBS) and stored as a cell pellet at −20 °C. The cell pellet from 8 dishes of cells was resuspended in 4 ml 1× Bind buffer (1 M NaCl, 20 mM Tris–HCl, 5 mM imidazole, pH 7.9), the cells lysed by sonication and the soluble protein extract collected by centrifugation at 18,500×*g* for 30 min at 4 °C. This extract was filtered and then applied to a 2.5 ml (bed volume) His.Bind column (Merck Biosciences Ltd., Nottingham, UK) charged with $NiSO_4$. The purification was performed according to the manufacturer's instructions, washing the column with 100 mM imidazole buffer prior to eluting the purified His-tagged PRPF31 off the column with 1× Elute buffer (1 M imidazole, 500 mM NaCl, 20 mM Tris–HCl, pH 7.9). A PD10 column (Amersham-Biosciences, Little Chalfont, UK) was then used to remove imidazole and effect buffer exchange to HEPES buffer (10 mM HEPES, 3.4 mM EDTA, 150 mM NaCl, 0.005% Tween, pH 7.4). Throughout the elution and buffer exchange steps, care was taken to minimise dilution of the protein, since downstream protein concentration using commercial microconcentrators always led to loss of product. Protein concentrations of all extracts were determined using a BioRad protein assay kit (BioRad Laboratories Ltd., Hemel Hempstead, UK) with γ-immunoglobulin as standard.

2.4. Purification of wild type and mutant His-tagged PRPF31 expressed in E. coli

E. coli strain Tuner (DE3) pLacI cells (Merck Biosciences Ltd., Nottingham, UK) were transformed with wild type or mutant pTriEx.PRPF31.His and grown in LB supplemented with chloramphenicol, ampicillin and 1% glucose to OD_{600} of 0.6–0.8. After induction with 0.1 mM IPTG, the cells were grown for a further 3 h at 37 °C before harvest. Inclusion bodies (containing insoluble His-tagged PRPF31) were isolated from a 200 ml aliquot of culture as described in

the His.Bind kit manual, including a lysozyme treatment. These were dissolved in 5 ml 1× Bind buffer containing 6 M urea for 1 h at 4 °C and centrifuged at 16,000×*g* for 30 min to remove insoluble material. The soluble extract was then filtered and applied to a 2.5 ml (bed volume) His.Bind column pre-charged with $NiSO_4$ and equilibrated with 1× Bind buffer containing 6 M urea. After washing with 1× Bind buffer (+6 M urea) and with 200 mM imidazole buffer (+6 M urea), the denatured, His-tagged PRPF31 was eluted off the column with 1× Elute buffer (+6 M urea). The protein concentration of the denatured protein extract was then reduced to 0.2 mg/ml with 1× Bind buffer (+6 M urea) and the extract dialysed in a Pierce Slide-A-Lyser cassette (PerBio Science UK Ltd., Cramlington, UK) against HEPES buffer containing reducing concentrations of urea. The protein concentration of the dialysed extract was around 0.1 mg/ml.

2.5. Purification of GST-tagged importin proteins

GST and GST-tagged Impα and Impβ were expressed from the above pGEX constructs in *E. coli* strain BL21 (DE3) cells. Liquid cultures were grown to log phase, induced with 0.1 mM IPTG and then grown overnight at 25 °C. In each case, the proteins were purified from a 20-ml aliquot of culture using a GST purification module (Amersham Biosciences, Little Chalfont, UK) and a batch procedure described in the manufacturer's instructions. 200 μl 50% glutathione sepharose slurry was used per purification and the GST-tagged protein was eluted off the resin using 2×250 μl reduced glutathione buffer. Glutathione was removed from the protein by passage through a PD10 column (Amersham Biosciences, Little Chalfont, UK), eluting with PBS. The purified protein was concentrated to at least 0.5 mg/ml using a YM10 Centricon column (Millipore (UK) Ltd. Watford, UK) passivated with 5% polyethylene glycol.

2.6. Pull-down assays

0.1 nmol of purified His-tagged PRPF31 or 10 units of human recombinant NF-κβ protein (Sigma-Aldrich, Poole, UK) were mixed with 0.1 nmol of purified GST-tagged importin protein or purified GST (negative control) in a total volume of 100 μl PBS. The mixture was rotated for 1 h at 4 °C. 20 μl of 50% glutathione sepharose beads were then added and rotation was continued for a further 30 min. The beads were centrifuged and washed 3 times with pre-chilled PBS. Bound proteins were eluted with 2×10 μl aliquots of reduced glutathione buffer. The combined fractions were mixed with SDS sample buffer and analysed by SDS-PAGE. Bound proteins were either stained with Coomassie or subjected to Western analysis as follows. Aliquots were separated in 12% SDS-PAGE gels and were then blotted on to Hybond ECL membrane (Amersham Biosciences, Little Chalfont, UK) using transfer buffer [50 mM Tris pH 9.1, 390 mM glycine, 0.04% SDS, 20% methanol]. Blots were blocked with 5% (w/v) dried milk proteins in PBS/0.1% Tween. For detection of His-tagged PRPF31 proteins, blots were probed with Penta.His antibody (Qiagen Ltd., Crawley, UK) at a dilution of 1:2000 followed, after washing, by an HRP-conjugated anti-mouse secondary antibody (Pierce Biochemicals Inc., Rochford, USA) at a dilution of 1:5000. For detection of NF-κβ, blots were probed with anti-NF-κB antibody (Merck Biosciences, Nottingham, UK) at a dilution of 1:500, followed after washing with an anti-rabbit HRP secondary antibody (Pierce Biochemicals Inc., Rochford, USA) at dilution of 1:15,000. Blots were developed with ECL-Plus HRP detection system (Amersham Biosciences, Little Chalfont, UK).

2.7. Western blot analyses of soluble cell lysates

Transfected HEK 293 T cells were harvested and sonicated in lysis buffer (20 mM HEPES pH 7.4, 0.4 mM EDTA, 450 mM NaCl, 0.5 mM DTT, 0.5 mM PMSF) to produce whole cell lysates. They were then spun at 13 K rpm in a chilled microfuge for 10 min and the soluble fractions removed to clean tubes. The protein contents of these soluble lysates were measured using a Biorad protein assay kit and were equalised by addition of further lysis buffer. Aliquots containing 10 μg protein were separated by SDS-PAGE electrophoresis, blotted and blocked as described above. Detection of His-tagged PRPF31 proteins was also as described above. For detection of EGFP-tagged PRPF31 proteins, blots were probed with an anti-EGFP monoclonal antibody (Abcam Ltd., Cambridge, UK) at a dilution of 1:5,000,000 followed by the same HRP-conjugated anti-mouse secondary antibody as used for the Penta.His antibody.

2.8. Fluorescence recovery after photobleaching (FRAP) analysis

COS7 cells were transfected with pPRPF31-EGFP constructs using GeneJuice in 3.5 cm glass bottom Microwell dishes (MatTek Corporation, Ashland, MA, USA) and grown for 24 h at 37 °C. 30 min prior to FRAP analysis the medium was changed to DMEM (without methyl red) supplemented with 50 μg/ml cyclohexiimide. Confocal imaging of EGFP-tagged proteins in the live cells was performed using a BioRad Radiance 2000 laser scanning microscope operated via Lasersharp v5.1 confocal imaging software and the Time-Course and Patterned Illumination option. The cells were visualised by a Zeiss Axiovert microscope using a Zeiss 63× Plan Apochromat oil immersion objective, a 488 nm laser-line excitation, and a narrow band 515–545 nm emission filter placed in front of the detector PMT. Image magnification could be further increased using the Bio-Rad optical zoom function (1 to 10×). All live-cell confocal imaging experiments were conducted at 37 °C in a thermostatically controlled incubator chamber, which was purged with 5% CO_2 in air and set up on the microscope XY stage. For FRAP analysis a region of interest (ROI) consisting of the area occupied by the nucleus at its widest point was selected. After a single pre-bleach imaging scan of the entire cell, the ROI was photobleached using 3 cycles of maximum laser power (50 mW) with $t=0$ s between cycles. The microscope was then immediately switched to imaging mode and time lapse sequences were recorded every 1 s for 10 cycles and then every 10 s for 20 cycles. Laser power used for imaging was <5% of maximum. Data acquisition was at 750 lines per second (lps) and each image was recorded twice and optimised using Kalman filtering (an averaging of sequential images to reduce noise). Control experiments in which an unbleached ROI was subjected to time lapse imaging under similar conditions indicated that photobleaching during normal data acquisition was not significant during the time course of the experiment. The kinetics of fluorescence recovery after nuclear photobleaching was determined from the variation in average fluorescence intensity in the ROI over time after photobleaching. Fluorescence intensities were normalised to the pre-bleach values, which were arbitrarily set to 1.

3. Results

3.1. Purification of wild type and mutant PRPF31.His proteins

Wild type and mutant PRPF31.His proteins were expressed as recombinant proteins in HEK 293 T cells. The wild type protein was purified to homogeneity (~95% purity) in a single step from a crude extract of soluble proteins from the cells using Ni^{2+} affinity chromatography (see Fig. 1a, lane 1). After desalting and buffer exchange, the maximum protein concentration achieved, however, was only around 0.1 mg/ml, and the purification of mutant protein A216P and A194E under the same conditions yielded very little protein (see Fig. 1a, lane 2). Attempts to increase protein yield using commercial protein concentrators were unsuccessful due to protein precipitation or adherence of protein to the membrane. We were, however, able to purify both wild type and mutant proteins under denaturing conditions from inclusion bodies to yield soluble denatured protein in good yield (Fig. 1a, lanes 3 and 4). When the denaturant was removed by dialysis, soluble renatured protein was obtained for both wild type and mutant in similar yield (Fig. 1a, lanes 5 and 6). Note, however, that it was necessary to reduce the protein concentration to less than 0.2 mg/ml during dialysis to minimise protein loss due to precipitation, and for the same reason, subsequent concentration of the renatured protein above ~0.1 mg/ml was not possible.

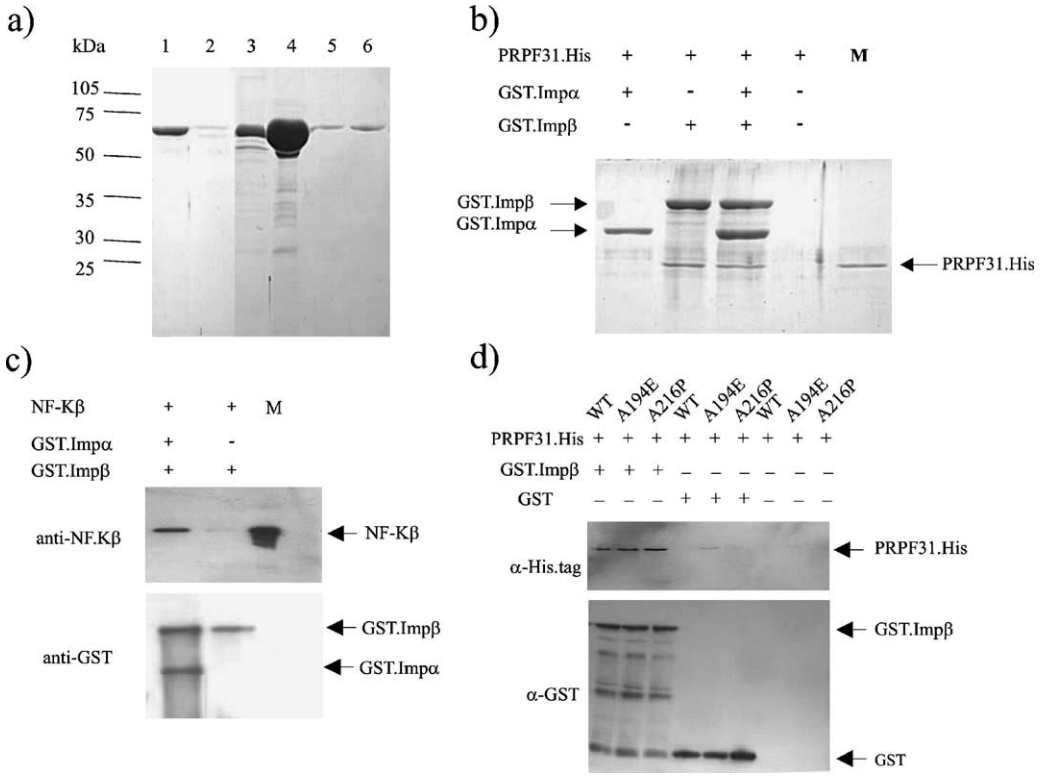

Fig. 1. Purification of PRPF31.His proteins and pull down assays with importin proteins. (a) Wild type (lane 1) and A216P mutant (lane 2) PRPF31 proteins expressed in HEK 293T cells and purified using His.bind columns under non-denaturing conditions, and wild type (lanes 3 and 5) and A216P mutant (lanes 4 and 6) proteins expressed in *E. coli* and purified from inclusion bodies by elution from His.bind columns (denatured—lanes 3 and 4) or after removal of denaturant by dialysis (soluble renatured proteins—lanes 5 and 6). (b) Coomassie blue stained SDS-PAGE gel showing binding of wild type PRPF31.His to GST-tagged importin β1 (lane 2), to an importin α1/importin β1 mixture (lane 3), but not to importin α1 alone (lane 1). (c) Western analysis of human recombinant NF-Kβ protein showing binding to an importin α1/importin β1 mixture (lane 1) but not to importin β1 alone (lane 2). Upper panel was probed with an NF-Kβ antibody and lower panel with α-GST antibody. (d) Western analysis of mutant PRPF31.His proteins after elution from immobilised GST-importin β1. Upper panel was probed with α-His.tag antibody and lower panel with α-GST antibody. M denotes marker lanes with purified proteins.

3.2. Importation of PRPF31 into the nucleus

PRPF31 contains a classical NLS but it is unknown which of the family of importin proteins is used to facilitate importation into the nucleus. Most proteins with classical NLSs interact with a heterodimer of importin α and importin β (reviewed in [10]). The NLS-binding site is on the α sub-unit, but binding is inhibited by an N-terminal sub-unit comprising the first 49 residues, which binds the β sub-unit. Binding of importin β relieves the inhibition and allows binding of the cargo protein via its NLS. Importin β is also responsible for translocation of the importin–cargo complex through the nuclear pore and, once inside the nucleus, importin β interacts with Ran-GTP to effect dissociation of the cargo protein into the nucleoplasm.

To examine the nuclear importation mechanism used for PRPF31, full-length human importin α1 and importin β1 were expressed with N-terminal GST tags in bacterial cells. The GST-tags were used to purify the proteins using glutathione-sepharose affinity chromatography. The importin proteins bound to glutathione-sepharose were then used to precipitate purified wild type PRPF31.His obtained from inclusion bodies and the precipitates were analysed by SDS PAGE with Coomassie blue staining (Fig. 1b). A band corresponding to PRPF31.His was seen using importin β1, both on its own (lane 2) and in combination with importin α1 (lane 3). As expected, importin α1 alone did not precipitate the PRPF31.His (lane 1). No detectable precipitation occurred in a control reaction without importin (lane 4), indicating that non-specific binding of the PRPF31.His to the glutathione-sepharose was minimal. These results indicate therefore that importation of PRPF31 into the nucleus involves binding to importin β1 alone with no absolute requirement for importin α1.

In order to confirm that recombinant importin α1 was active in binding target proteins, the experiments were repeated with human recombinant NF-κβ, a transcription factor that is a known target for importin α [13]. As shown in Fig. 1c, NF-κβ was recovered in pull-down assays with an importin α1/importin β1 mixture (lane 1), but not with importin β1 alone (lane 2), demonstrating therefore the functionality of importin α1 and that importin β1 does not bind non-specifically.

Binding of wild type and mutant PRPF31.His to GST-importin β1 was compared using similar pull-down assays, but in this case gels were blotted and probed with anti-His.tag and anti-GST.tag antibodies for the detection step (Fig. 1d). The A194E and A216P mutations did not appear to affect binding to GST-importin β1. Control reactions with GST protein alone

were negative indicating that non-specific binding of both wild type and mutant PRPF31.His to the GST tag was negligible.

3.3. Effect of purification tags on expression and solubility of PRPF31

Our previous studies have indicated that, when expressed with a His-tag, the A194E and A216P mutations resulted in protein insolubility compared to wild type [8]. In contrast, the following experiment shows that, when wild type and mutant PRPF31 are expressed in HEK 293T cells with a C-terminal EGFP-tag, this solubility difference is lost. Whole cell extracts and soluble cell extracts of both His-tagged and EGFP-tagged proteins were subjected to Western analysis using anti-His tag and anti-EGFP tag antibodies, respectively (Fig. 2). When band strength was quantified using Genesnap software (Syngene), this indicated that the ratio of soluble to total expressed PRPF31 protein was substantially lower for the His-tagged mutant proteins than for wild type (0.72 (WT), 0.39 (A194E mutant) and 0.24 (A216P mutant)) whereas the ratios for the EGFP-tagged proteins were comparable (0.87 (WT), 0.80 (A194E mutant) and 0.90 (A216P mutant)). Indeed, the results showed that whereas the His-tagged proteins remain largely in the insoluble fraction, nearly all the expressed EGFP-tagged protein was recovered in a soluble form.

3.4. Real-time study of nuclear importation of PRPF31

Wild type and mutant EGFP-tagged PRPF31 were expressed in COS7 cells and examined directly in live cells using a Bio-Rad Radiance 2000 confocal microscope fitted with a 488-nm line excitation laser. When the cells were examined at 24 h post-transfection both wild type and mutant proteins were present in the nucleus with only a faint fluorescent signal from the cytoplasm. The cells appeared healthy with well-rounded nuclei.

Fluorescence recovery after photobleaching (FRAP), a dynamic cell imaging technique, was used to examine the actual rate of importation of PRPF31-EGFP into the nucleus in these live transfected cells [14,15]. Nuclei were selectively photobleached by scanning with the Radiance 488 nm laser; the subsequent recovery of fluorescence within these nuclei is due to movement of unbleached PRPF31-EGFP from the cytoplasm. This recovery was recorded by sequential scanning of the cell (as shown in Fig. 3a). The recovery of cells expressing EGFP alone is also shown for comparison. Since the amount of PRPF31-EGFP present in the cytoplasm at the start of the experiment is much lower than for EGFP itself, the relative recovery is much smaller than the latter but is nonetheless measurable and reproducible.

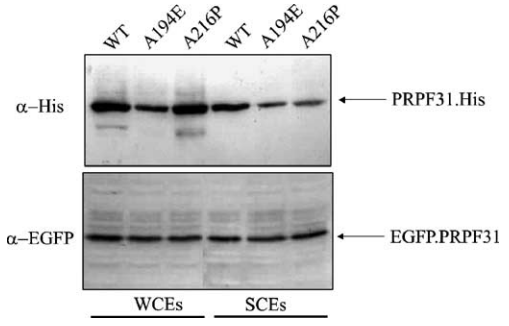

Fig. 2. Comparison of protein solubility of His-tagged and EGFP-tagged PRPF31 proteins expressed in HEK 293T cells. Whole cell extracts (WCEs) and soluble cell extracts (SCEs) containing equivalent amounts of total protein were subjected to western analysis using α-His.tag (upper panel) and α-EGFP (lower panel) monoclonal antibodies.

The kinetics of fluorescence recovery due to protein transport across the nuclear membrane was measured after photobleaching a region of interest (ROI), which in this case comprised the whole nucleus. Before photobleaching, the mean fluorescence intensity over the ROI was measured and photobleaching within the ROI was then achieved using 3 rapid cycles of 100% intensity 488 nm laser light. Sequential confocal images of the entire cell were then taken, initially at 1-s intervals for 10 cycles, followed by a further 20 cycles at 10 s intervals. This FRAP protocol was adopted because the initial recovery of fluorescence was very fast, necessitating fast data acquisition, whilst the later stages could be tracked using a longer cycle time. In this way pigment photobleaching as a result of sequential scanning was minimised and indeed was found to be negligible in control experiments.

Fluorescence intensity data from these images were used to measure nuclear fluorescence recovery as a function of time (Fig. 3b). FRAP data were normalised to the pre-bleach values, which were arbitrarily set to 1. The time course of recovery was fitted to a standard FRAP recovery equation: $I=A^*(1-\exp(-t/\tau))+I_o$, where I is the nuclear fluorescence intensity, I_o is the nuclear fluorescence at the start of recovery, A is a scaling constant and τ is the recovery time constant. This failed to provide an adequate fit to the early stages of the recovery, when the rate of fluorescence recovery was fastest (Fig. 3b(i)). We thus investigated the possibility that the rate of recovery might include two components, a fast component dominating the early stages of the recovery and a slower component, which became significant in the later stages. The standard FRAP equation was thus fitted to the first 10 data points to provide a theoretical 'fast' FRAP curve. This was then deducted from all the experimental data points which were then fitted with a 'slow' FRAP curve. The combined 'fast+slow' theoretical curve then provided a satisfactory fit to the experimental data (Fig. 3b(ii)).

Using this method recovery time constants, τ_{fast} and τ_{slow}, were derived from the data for each cell measured and are presented in Table 1. The recovery time constant for the slow component of wild type PRPF31-EGFP importation (78.4±25.4 s) was comparable to the value obtained for the EGFP control (99.5±1.9 s). In contrast the value for the fast component of wild type PRPF31-EGFP importation was at least 12-fold faster (6.31±0.08 s). The values obtained for the two mutant proteins were not significantly different from the wild type values for both fast and slow components (Fig. 3b(iii), (iv) and Table 1).

4. Discussion

In this study, the mechanism of importation of the splicing factor protein PRPF31 into the nucleus and the impact of two

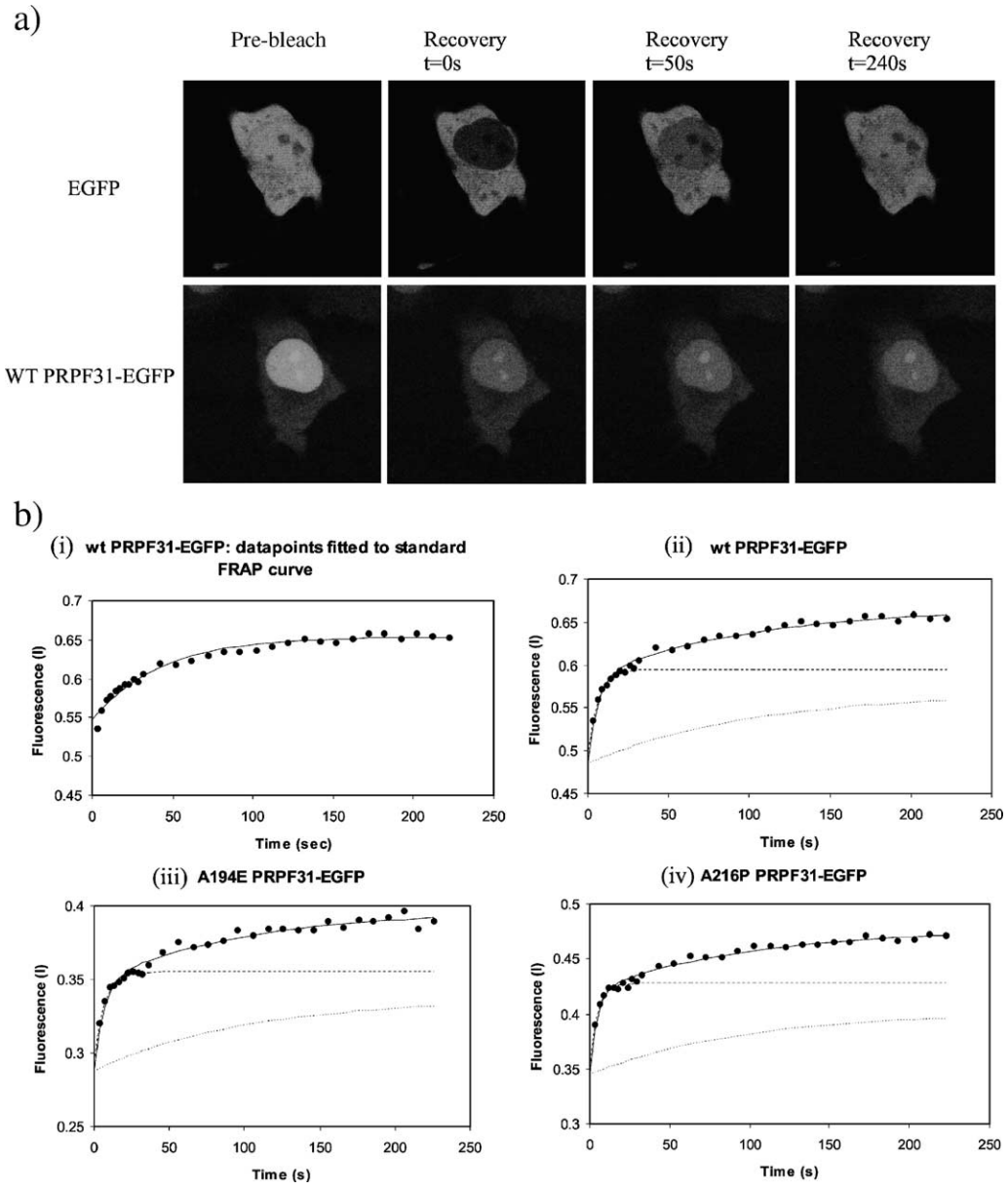

Fig. 3. FRAP analysis of importation of wild type and mutant PRPF31 proteins into the nuclei of transfected COS7 cells. (a) Confocal images show single z sections of cells expressing EGFP and wild type PRPF31-EGFP pre-bleach and at the indicated time points post-bleach. (b) Kinetics of fluorescence recovery after nuclear photobleaching. Datapoints for wild type PRPF31-EGFP failed to fit a standard FRAP recovery curve of form $I=A*(1-\exp(-t/\tau))+Io$ (i) but fitted a two component recovery curve (ii) as described in Results.

missense mutations, A194E and A216P, on this process have been examined. In order to investigate the interaction of PRPF31 with proteins from the importin family, the first step was to purify the wild type protein and the two mutant variants. A His-tag was used to simplify the purification, but attempts to purify both the wild type and more particularly the mutant proteins were complicated by protein insolubility and aggregation. Wild type and mutant proteins were eventually purified under denaturing conditions and found to re-fold as soluble proteins on removal of denaturant. Efforts to concentrate the proteins above 0.1 mg/ml were unsuccessful, however, due to protein precipitation.

Table 1
Time constants (τ) for recovery of nuclear fluorescence (mean±standard deviation, $n=3$) (s)

PRPF31-EGFP			EGFP
WT	A194E	A216P	
$\tau_{fast}=6.31\pm0.08$ $\tau_{slow}=78.4\pm25.4$	$\tau_{fast}=5.66\pm0.69$ $\tau_{slow}=77.1\pm22.4$	$\tau_{fast}=5.68\pm0.97$ $\tau_{slow}=83.3\pm13.5$	$\tau=99.5\pm1.9$

The results of the solubility study indicate that the nature of the purification tag affects protein solubility. In particular, the reduced solubility of mutant protein when expressed with a small His-tag is not seen when expressed with the much larger 24 kDa EGFP protein tag. Moreover, the wild type protein is more soluble with an EGFP tag, which leads us to suspect that the addition of this relatively large protein to PRPF31 has the

general effect of promoting solubility and eliminating solubility differences between the wild type and mutant forms. It is at present unknown whether untagged mutant PRPF31 gives rise to solubility problems in the photoreceptors of ADRP patients but we would propose that the smaller His-tagged version is more likely to behave like the untagged protein than the version with the much larger EGFP-tag.

Although we cannot rule out the binding of PRPF31 to importin α/β heterodimers [10], the finding that PRPF31 interacts directly with importin β1 was unexpected in view of its possession of what appears to be a classical NLS. Certain transport substrates have been reported to bind directly to importin β in the absence of importin α, for example PTHrP [16], HIV-1 [17] and hnRNP binding proteins [18], but no clear consensus sequence for this binding has emerged. This finding should contribute to the definition of the consensus NLSs required for binding directly to importin β as compared to importin α/β heterodimers.

Previous studies have indicated that proteins of molecular size up to 56 kDa are able to move through the nuclear pores freely by passive diffusion, but that larger proteins require the assistance of nuclear importation machinery involving both the importins and Ran-GTP in an energy-dependent process [15]. Using the FRAP technique, movement of EGFP, a protein of 24 kDa, was shown to be by passive diffusion and was independent of cellular GTP or ATP. However, the movement was slowed ~100 fold compared to diffusion within the nucleus or cytoplasm due to the reduced cross-sectional areas of the nuclear pores themselves [15]. The rate of nuclear importation of EGFP measured in this study (τ ~99 s) is rather faster than previously reported [15], possibly due to experimental differences between laboratories using this novel technique, but is broadly consistent with the previous finding. In contrast the size of the EGFP-tagged PRPF31 protein precludes passive diffusion. The FRAP analysis of the nuclear importation of this protein indicated a two component recovery process, a fast component with kinetics comparable to that for free diffusion within an unbounded compartment ($\tau \sim 6$ s), and a slow component with kinetics comparable to that for passive diffusion through the nuclear pores ($\tau \sim 80$ s). Which of these components represents the importin-assisted passage across the nuclear membrane? The fast component is similar in magnitude to the rate of passive diffusion across an unbounded space and may thus be attributable to movement of unbleached pigment surviving the photobleaching step from remote areas within the nucleus. Therefore, the slow component most likely represents the rate of movement through the nuclear pores. The magnitude of this rate might suggest that the number and size of the nuclear pores is the factor controlling the rate of nuclear transport, whether that process is active or passive.

The experiments presented here are consistent in showing that the mutant proteins are able to interact with importin and that the rate of importation of the soluble forms of the wild type and mutant proteins into the nucleus is the same. This result re-affirms therefore the importance of the mutant protein insolubility in the development of disease pathology. Our previous studies [8] on PRPF31 have shown that, when expressed as His-tagged proteins, these two mutations cause an accumulation of mutant protein in the cytoplasm, presumably as a direct result of protein insolubility, with reduced levels in the nucleus. The overall consequence of this would be a reduction in the level of functional protein in the nucleus. In rod photoreceptor cells, with a very high demand for protein synthesis, this could result in an insufficiency of splicing activity. Consistent with this explanation is the finding that retina-derived primary cultures that express mutant PRPF31 proteins contain reduced concentrations of rhodopsin, normally the most abundant protein in such cells [9]. The incomplete penetrance that is common in this form of RP [19] would also fit this hypothesis: the overall level of PRPF31 production is determined by variants of the gene that determine transcription activity, so a high or low production of normal gene product from the normal allele will result respectively in more or less splicing capability in photoreceptors and the absence or presence of pathology.

Schaffert et al. [20] recently showed using PRPF31 knock-down experiments on live cells that, once inside the nucleus, PRPF31 cycles between nuclear speckles (the sites of splicing factor storage), the Cajal bodies (the sites of tri-snRNP assembly) and the nucleoplasm, and that in the absence of PRPF31, U4/U6 di-snRNPs and p110 accumulate in the Cajal bodies, whereas U5 snRNPs largely remain in the speckles. It will be interesting to discover whether the A194E and A216P mutations have any effect on this cycling of PRPF31 or on the pattern of accumulation of other factors within the nucleus.

Acknowledgements

We are grateful to A. I. Lamond (University of Dundee, UK) for the importin α construct, pRSET-hSRP1α, and to K. Weis (University of Berkeley, USA) for the importin β construct, pET30b.Impβ. This work was supported by the British Retinitis Pigmentosa Society, the Wellcome Trust, Fight for Sight and by a Value in People award to SEW from University College London.

References

[1] E.N. Vithana, L. Abu-Safieh, M.J. Allen, A. Carey, M. Papaioannou, C. Chakarova, M. Al-Maghtheh, N.D. Ebenezer, C. Willis, A.T. Moore, A.C. Bird, D.M. Hunt, S.S. Bhattacharya, A human homolog of yeast pre-mRNA splicing gene, PRP31, underlies autosomal dominant retinitis pigmentosa on chromosome 19q13.4 (RP11), Mol. Cell 8 (2001) 375–381.

[2] A.B. McKie, J.C. McHale, T.J. Keen, E.E. Tarttelin, R. Goliath, J.J. van Lith-Verhoeven, J. Greenberg, R.S. Ramesar, C.B. Hoyng, F.P. Cremers, D.A. Mackey, S.S. Bhattacharya, A.C. Bird, A.F. Markham, C.F. Inglehearn, Mutations in the pre-mRNA splicing factor gene PRPC8 in autosomal dominant retinitis pigmentosa (RP13), Hum. Mol. Genet. 10 (2001) 1555–1562.

[3] C.F. Chakarova, M.M. Hims, H. Bolz, L. Abu-Safieh, R.J. Patel, M.G. Papaioannou, C.F. Inglehearn, T.J. Keen, C. Willis, A.T. Moore, T. Rosenberg, A.R. Webster, A.C. Bird, A. Gal, D. Hunt, E.N. Vithana, S.S. Bhattacharya, Mutations in HPRP3, a third member of pre-mRNA splicing factor genes, implicated in autosomal dominant retinitis pigmentosa, Hum. Mol. Genet. 11 (2002) 87–92.

[4] O.V. Makarova, E.M. Makarov, S. Liu, H.P. Vornlocher, R. Luhrmann, Protein 61K, encoded by a gene (PRPF31) linked to autosomal dominant

retinitis pigmentosa, is required for U4/U6*U5 tri-snRNP formation and pre-mRNA splicing, EMBO. J. 21 (2002) 1148–1157.
[5] E.M. Makarov, O.V. Makarova, H. Urlaub, M. Gentzel, C.L. Will, M. Wilm, R. Luhrmann, Small nuclear ribonucleoprotein remodeling during catalytic activation of the spliceosome, Science 298 (2002) 2205–2208.
[6] C.L. Will, R. Luhrmann, Spliceosomal UsnRNP biogenesis, structure and function, Curr. Opin. Cell Biol. 13 (2001) 290–301.
[7] Z. Zhou, L.J. Licklider, S.P. Gygi, R. Reed, Comprehensive proteomic analysis of the human spliceosome, Nature 419 (2002) 182–185.
[8] E.C. Deery, E.N. Vithana, R.J. Newbold, V.A. Gallon, S.S. Bhattacharya, M.J. Warren, D.M. Hunt, S.E. Wilkie, Disease mechanism for retinitis pigmentosa (RP11) caused by mutations in the splicing factor gene PRPF31, Hum. Mol. Genet. 11 (2002) 3209–3219.
[9] L. Yuan, M. Kawada, N. Havlioglu, H. Tang, J.Y. Wu, Mutations in PRPF31 inhibit pre-mRNA splicing of rhodopsin gene and cause apoptosis of retinal cells, J. Neurosci. 25 (2005) 748–757.
[10] D.A. Jans, C.Y. Xiao, M.H. Lam, Nuclear targeting signal recognition: a key control point in nuclear transport? BioEssays 22 (2000) 532–544.
[11] K. Weis, I.W. Mattaj, A.I. Lamond, Identification of hSRP1 alpha as a functional receptor for nuclear localization sequences, Science 268 (1995) 1049–1053.
[12] N.C. Chi, E.J. Adam, S.A. Adam, Sequence and characterization of cytoplasmic nuclear protein import factor p97, J. Cell Biol. 130 (1995) 265–274.
[13] S.G. Nadler, D. Tritschler, O.K. Haffar, J. Blake, A.G. Bruce, J.S. Cleaveland, Differential expression and sequence-specific interaction of karyopherin α with nuclear localization sequences, J. Biol. Chem. 272 (1997) 4310–4315.
[14] J. White, E. Stelzer, Photobleaching GFP reveals protein dynamics inside live cells, Trends Cell. Biol. 9 (1999) 61–65.
[15] X. Wei, V.G. Henke, C. Strubing, E.B. Brown, D.E. Clapham, Real-time imaging of nuclear permeation by EGFP in single intact cells, Biophys J. 84 (2003) 1317–1327.
[16] M.H. Lam, L.J. Briggs, W. Hu, T.J. Martin, M.T. Gillespie, D.A. Jans, Importin beta recognizes parathyroid hormone-related protein with high affinity and mediates its nuclear import in the absence of importin alpha, J. Biol. Chem. 274 (1999) 7391–7398.
[17] R. Truant, B.R. Cullen, The arginine-rich domains present in human immunodeficiency virus type 1 Tat and Rev function as direct importin beta-dependent nuclear localization signals, Mol. Cell. Biol. 19 (1999) 1210–1217.
[18] H. Siomi, P. Eder, N. Kataoka, L. Wan, Q. Liu, G. Dreyfuss, Transportin-mediated nuclear import of heterogeneous nuclear RNP proteins, J. Cell Biol. 138 (1997) 1181–1192.
[19] E.N. Vithana, L. Abu-Safieh, L. Pelosini, E. Winchester, D. Hornan, A.C. Bird, D.M. Hunt, S.A. Bustin, S.S. Bhattacharya, Expression of PRPF31 mRNA in patients with autosomal dominant retinitis pigmentosa: a molecular clue for incomplete penetrance? Investig. Ophthalmol. Vis. Sci. 44 (2003) 4204–4209.
[20] N. Schaffert, M. Hossbach, R. Heintzmann, T. Achsel, R. Luhrmann, RNAi knockdown of hPrp31 leads to an accumulation of U4/U6 di-snRNPs in Cajal bodies, EMBO J. 23 (2004) 3000–3009.